

AD-A145 104

IMPEDANCE MEASUREMENTS ON A VLF MULTI-TURN LOOP ANTENNA 1//
IN A SPACE PLASMA..(U) AEROSPACE CORP EL SEGUNDO CA
SPACE SCIENCES LAB H C KOONS ET AL. 15 JUN 84

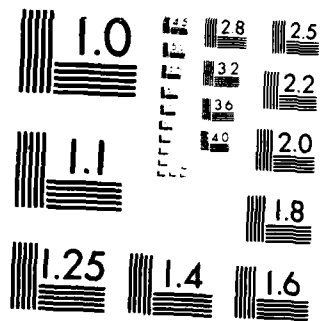
UNCLASSIFIED

TR-0084(4723)-1 SD-TR-84-21

F/G 9/5

NL

END
DATE
FILED
9 84
DTIC



MICROCOPY RESOLUTION TEST CHART
NATIONAL BUREAU OF STANDARDS 1963-A

12

AD-A145 104

Impedance Measurements on a VLF Multi-Turn Loop Antenna in a Space Plasma Simulation Chamber

H. C. KOONS, M. H. DAZEY, and B. C. EDGAR
Space Sciences Laboratory
Laboratory Operations
The Aerospace Corporation
El Segundo, Calif. 90245

15 June 1984

APPROVED FOR PUBLIC RELEASE;
DISTRIBUTION UNLIMITED

Prepared for
NAVAL AIR SYSTEMS COMMAND
Arlington, Va. 20360

DTIC FILE COPY

DTIC
ELECTE
AUG 28 1984
A B

SPACE DIVISION
AIR FORCE SYSTEMS COMMAND
Los Angeles Air Force Station
P.O. Box 92960, Worldway Postal Center
Los Angeles, Calif. 90009

84 08 27 156

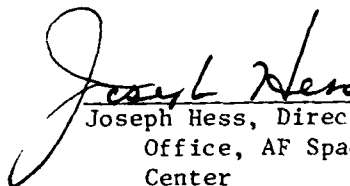
This report was submitted by The Aerospace Corporation, El Segundo, CA 90245, under Contract No. F04701-83-C-0084 with the Space Division, P.O. Box 92960, Worldway Postal Center, Los Angeles, CA 90009. It was reviewed and approved for The Aerospace Corporation by H. R. Rugge, Director, Space Sciences Laboratory. Lt Douglas R. Case, SD/YCM, was the project officer for the Mission Oriented Investigation and Experimentation Program.

This report has been reviewed by the Public Affairs Office (PAS) and is releasable to the National Technical Information Service (NTIS). At NTIS, it will be available to the general public, including foreign nationals.

This technical report has been reviewed and is approved for publication. Publication of this report does not constitute Air Force approval of the report's findings or conclusions. It is published only for the exchange and stimulation of ideas.



Douglas R. Case, Lt, USAF
Project Officer



Joseph Hess, Director, West Coast
Office, AF Space Technology
Center

UNCLASSIFIED

SECURITY CLASSIFICATION OF THIS PAGE (When Data Entered)

REPORT DOCUMENTATION PAGE		READ INSTRUCTIONS BEFORE COMPLETING FORM
1. REPORT NUMBER SD-TR-84-21	2. GOVT ACCESSION NO. AD-4145 104	3. RECIPIENT'S CATALOG NUMBER
4. TITLE (and Subtitle) IMPEDANCE MEASUREMENTS ON A VLF MULTI-TURN LOOP ANTENNA IN A SPACE PLASMA SIMULATION CHAMBER		5. TYPE OF REPORT & PERIOD COVERED
7. AUTHOR(s) Harry C. Koons, Mitchell H. Dazey, and Bruce C. Edgar		6. PERFORMING ORG. REPORT NUMBER TR-0084 (4723)-1
9. PERFORMING ORGANIZATION NAME AND ADDRESS The Aerospace Corporation El Segundo, Calif. 90245		8. CONTRACT OR GRANT NUMBER(s) FO4701-83-C-0084
11. CONTROLLING OFFICE NAME AND ADDRESS Naval Air Systems Command Arlington, Va. 20360		10. PROGRAM ELEMENT, PROJECT, TASK AREA & WORK UNIT NUMBERS
14. MONITORING AGENCY NAME & ADDRESS (if different from Controlling Office)		12. REPORT DATE 15 June 1984
		13. NUMBER OF PAGES 23
		15. SECURITY CLASS. (of this report) Unclassified
		15a. DECLASSIFICATION/DOWNGRADING SCHEDULE
16. DISTRIBUTION STATEMENT (of this Report) Approved for public release; distribution unlimited.		
17. DISTRIBUTION STATEMENT (of the abstract entered in Block 20, if different from Report)		
18. SUPPLEMENTARY NOTES		
19. KEY WORDS (Continue on reverse side if necessary and identify by block number)		
20. ABSTRACT (Continue on reverse side if necessary and identify by block number) The Space Sciences Laboratory of The Aerospace Corporation is presently defining an experiment to test a loop antenna configuration for a VLF transmitter in the ionosphere. The primary objectives of the experiment are to validate existing models for radiation by a loop antenna and to study the performance of the antenna in the ionospheric plasma. A one-third scale model of the antenna has been constructed. Impedance measurements have been made on the model in a 5-m diameter space plasma simulation chamber at NASA		

DD FORM 1473
(FACSIMILE)

UNCLASSIFIED

SECURITY CLASSIFICATION OF THIS PAGE (When Data Entered)

UNCLASSIFIED

SECURITY CLASSIFICATION OF THIS PAGE(When Data Entered)

19. KEY WORDS (Continued)

20. ABSTRACT (Continued)

Lewis Research Center. The measurements confirm that the reactance of the antenna in an ionospheric plasma is essentially identical to its free space self inductance. The effective series resistance of the circuit increases with frequency. The losses are attributed to power transferred to plasma turbulence.

UNCLASSIFIED

SECURITY CLASSIFICATION OF THIS PAGE(When Data Entered)

PREFACE

We are indebted to L. Corpas, B. Vetrone, N. Grier and the NASA Lewis Research Center personnel who lent their ready assistance to us for the tests performed at their facility.

We would like to thank B. Baldree from Aerospace for his help with the tests. We would also like to thank B. Holzworth for his efforts in locating a suitable vacuum chamber for the tests.

S **DTIC**
ELECTE **D**
AUG 28 1984
B

Accession For	
NTIS GRA&I	<input checked="checked" type="checkbox"/>
DTIC TAB	<input type="checkbox"/>
Unannounced	<input type="checkbox"/>
Justification	
By	
Distribution/	
Availability codes	
Avail. and/or	
Dist	Special
A-1	



CONTENTS

PREFACE.....	1
INTRODUCTION.....	9
PLASMA CHAMBER TESTS.....	10
RESULTS.....	12
SUMMARY.....	19
REFERENCES.....	21

FIGURES

1.	Antenna Current as a Function of Frequency at Two Voltage Levels.....	13
2.	Resonant Frequency of the Antenna Circuit as a Function of the Angle Between the Antenna Axis and the Imposed External Magnetic Field for the Antenna in Vacuum and at Plasma Densities of 5×10^4 and $1 \times 10^6 \text{ cm}^{-3}$ for Three Different Values of the Tuning Capacitance: (a) 79 μf , (b) 22 μf , and (c) 6.3 μf	14
3.	Histogram of the Antenna Circuit Series Resistance at Resonance for the Five Frequencies and Three Plasma Conditions Used in the Plasma Chamber Tests.....	15
4.	Wave Spectrum in Plasma in the Frequency Range from 0 to 20 MHz.....	18

TABLES

1. Scale-Model Antenna Parameters.....	11
2. Drive Current in Amps r.m.s. for the Data Shown in Fig. 3.....	16

PREVIOUS PAGE
IS BLANK

Introduction

The theory for the impedance, the radiation resistance, and the radiation pattern for both dipole and loop antennas at VLF in a plasma was formulated in the early 1970's [Wang and Bell, 1970, 1972; Bell and Wang, 1971].

Measurements of the impedance of electric dipole antennas in the low voltage linear regime have been performed using both rocket and satellite probes [Liephart et al., 1962; Shawhan and Gurnett, 1968; Grard and Tunaley, 1968; Gurnett et al., 1969; Koons et al., 1970]. These measurements showed that the impedance of the plasma sheath surrounding the antenna elements dominated the impedance at the antenna terminals. Shkarofsky [1972] developed a quasistatic nonlinear sheath model which he used to compute the impedance of an electric-dipole antenna driven at voltages much larger than plasma potential.

Measurements of the nonlinear impedance were made on a 32-m dipole at voltages up to 100 V peak-to-peak at seven frequencies from 400 Hz to 14 kHz on the OV1-21 satellite by Koons and McPherson [1974]. The magnitude of the impedance was in excellent agreement with Shkarofsky's model. However, the phase was found to advance with increasing voltage drive and increasing frequency. This phase advance implied an inductive reactance in the circuit. This result was contrary to existing nonlinear sheath models which predicted an increasing capacitive reactance as frequency and voltage increase [Shkarofsky, 1972; Baker et al., 1973].

The conclusion from the OV1-21 impedance measurements was that an electric-dipole antenna could not be resonated using a fixed reactance because nonlinear plasma effects caused significant changes in the impedance of the



antenna circuit on a time scale that is shorter than the period of the applied signal. The theory for a loop antenna in an ionospheric plasma predicts that the resonant frequency will only shift about 1 part in 10^4 [Wang and Bell, 1972].

Plasma Chamber Tests

A scale-model loop antenna was operated in a 5-m diameter space plasma simulation chamber at the NASA Lewis Research Center. The antenna parameters are listed in Table 1. The objectives of the test were to measure the absolute value of the complex impedance, the resonant frequencies, and the near fields of the antenna. The thermal properties of the structure and plasma instabilities generated by the VLF fields were also measured.

The measurements were made in an argon ion plasma under two conditions. A relatively uniform density of 8×10^4 elec/cm³ was produced using four plasma guns. A higher density of 1.2×10^6 elec/cm³ was produced at the antenna by augmenting the plasma guns with a plasma thruster at one end of the chamber. The thruster produced a directed flow along the axis of the chamber with a density gradient of 10^6 elec/cm³/m. The electron density and temperature were measured by four Langmuir probes placed about the antenna. In the low density plasma the electron temperature was 1.1 eV. In the high density plasma the temperature was 0.6 eV. Helmholtz coils provided a 0.4 G field parallel to the axis of the cylindrical vacuum chamber.

Table 1. Scale-Model Antenna Parameters

Diameter	110 cm
Height	66 cm
Weight	60.5 kg
Copper Tubing	3/8 in O. D.
Turns	37
Structural Material	Lexan

Results

One of the major results of the measurements was the confirmation that the resonant frequency of the tuned antenna circuit is insensitive to the plasma density. Fig. 1 shows typical resonances in the antenna current for the antenna in the plasma. These measurements were made by sweeping the frequency at a constant amplifier voltage. Below a plasma wave instability threshold a smooth curve is obtained. Above that threshold, which occurs at an antenna current of 8.6 A r.m.s. in Fig. 1, the circuit resistance abruptly increases. There is only a slight shift in the resonant frequency. The resonant frequency for three different values of the tuning capacitance is shown in Fig. 2. Even in the absence of the plasma the resonant frequency depends upon the orientation of the antenna in the tank. The resonant frequency is slightly lower when the axis of the antenna is perpendicular to the axis of the tank. At 500 Hz the shift in the resonant frequency is smaller than the resolution (~ 5 Hz) of the measuring instruments over the entire range of plasma densities and antenna orientations. At 7000 Hz there is a shift of about 20 Hz or 3 parts in 10^3 at the highest density.

The series resistance of the circuit at resonance is the r.m.s. voltage divided by the r.m.s. current. The histogram in Fig. 3 shows this series circuit resistance as a function of frequency for the antenna in vacuum and for the two plasma densities. Table 2 shows the drive current for each condition. At the lower frequencies the resistance is almost unaffected by the plasma. At the higher frequencies the resistance increases as the density increases.

Using available tuning capacitors, the resonant frequency of the circuit

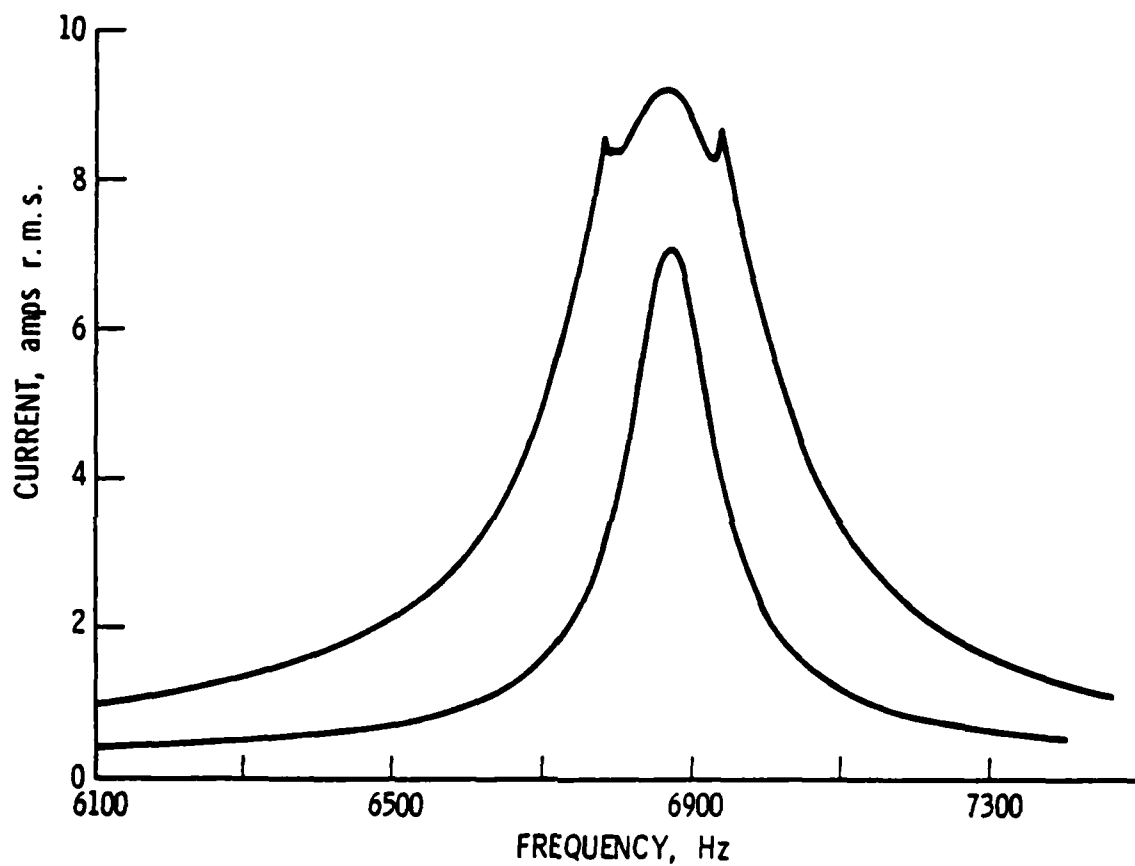


Fig. 1. Antenna current as a function of frequency at two voltage levels.
The higher current curve shows the result of a sudden change of the Q
of the resonance circuit at about 8.5 A.

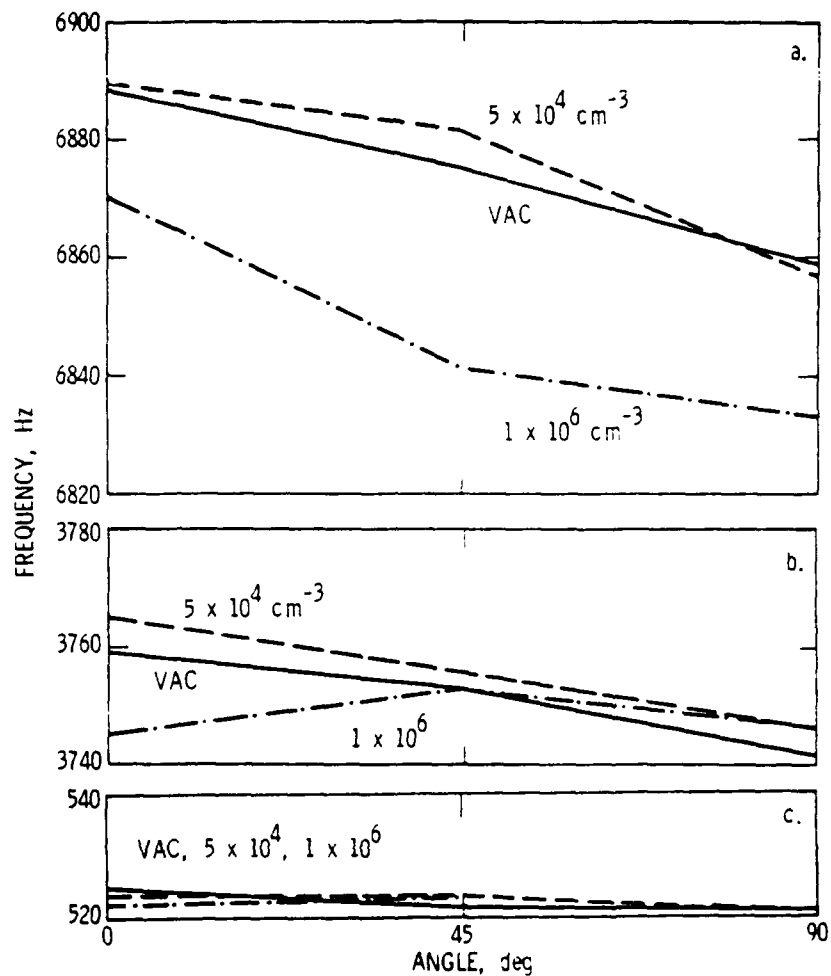


Fig. 2 Resonant frequency of the antenna circuit as a function of the angle between the antenna axis and the imposed external magnetic field for the antenna in vacuum and at plasma densities of 5×10^4 and $1 \times 10^6 \text{ cm}^{-3}$ for three different values of the tuning capacitance: (a) 79 μf , (b) 22 μf , and (c) 6.3 μf .

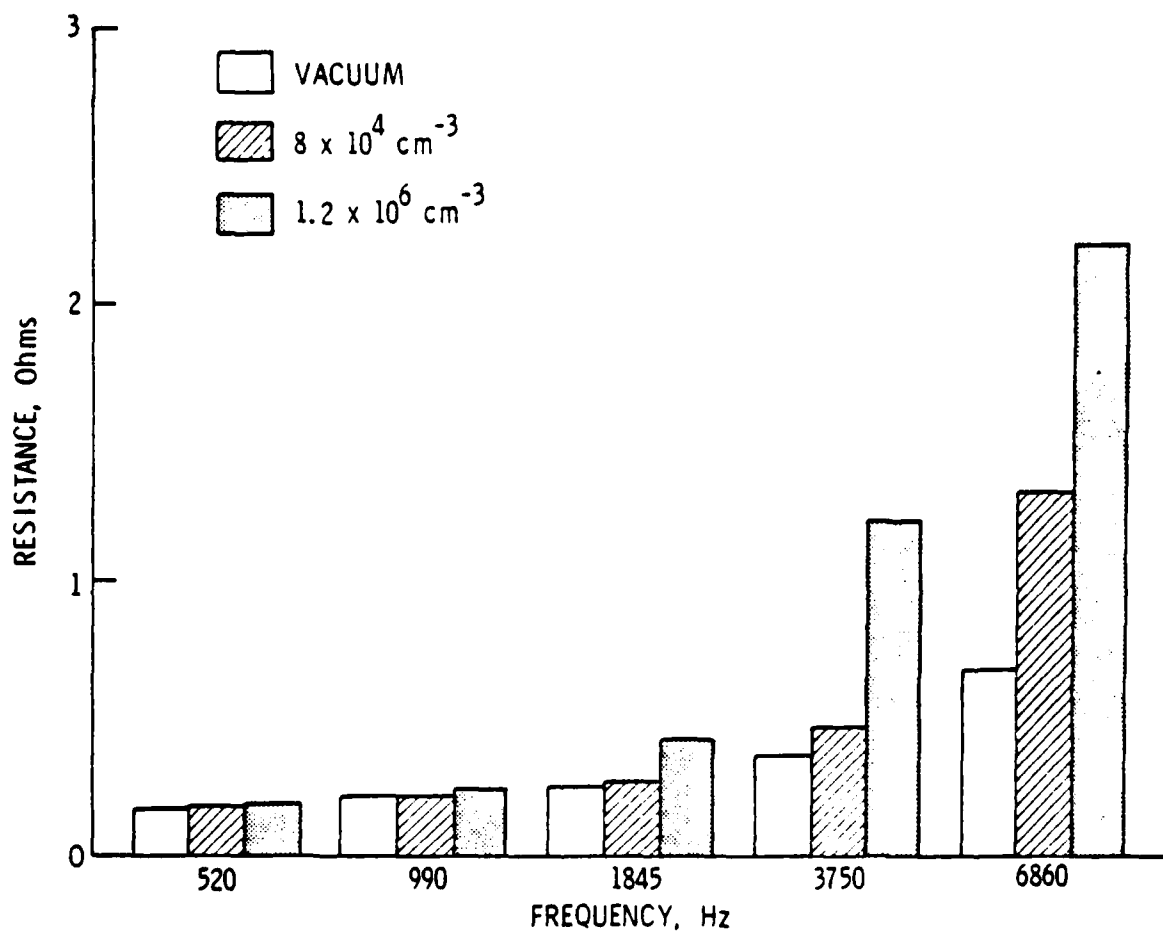


Fig. 3 Histogram of the antenna circuit series resistance at resonance for the five frequencies and three plasma conditions used in the plasma chamber tests.

Table 2. Drive current in Amps r.m.s.
for the data shown in Fig. 3

	FREQUENCY, Hz				
	500	990	1845	3750	6860
Vacuum	27.0	23.5	21.4	14.0	10.4
8×10^4	25.2	25.1	23.4	23.4	10.1
1.2×10^6	25.5	25.0	24.1	11.1	5.7

could only be changed in discrete steps that were approximately an octave apart. For this reason it was not possible to sweep in frequency to look for impedance effects near the lower-hybrid-resonance frequency (LHR). The LHR was 3.7 kHz at the lower density and 4.1 kHz at the higher density. The data in Fig. 3 suggest that the increase in series resistance may in part be related to the LHR. Well below the LHR the resistance was insensitive to density, while above the LHR, in the frequency range where the index of refraction has a resonance cone, the resistance increased with density. This large increase in series resistance is not predicted by existing theory [Wang and Bell, 1972].

The increase in circuit resistance was accompanied by an increase in plasma turbulence. Fig. 4 shows the plasma wave spectrum from 0 to 20 MHz on a small electric field probe in the plasma. The data were taken at a nominal electron density of 1.2×10^6 elec/cm³. Fig. 4a shows the background spectrum in the plasma in the absence of antenna current.

The line near 9 MHz in Fig. 4a and 12 MHz in Fig. 4b is an EMI line that is not related to the antenna measurements. The feature from 14 to 16 MHz appears when the plasma thruster is turned on. It is most likely related to the plasma frequency in the higher density region near the aperture of the thruster.

Fig. 4b shows the spectrum with the VLF antenna carrying 22.4 A at 1843 Hz. The broad feature near 9 MHz peaks near the plasma frequency. The "picket fence" structure in the spectrum is an artifact of the data presentation. The sweep rate of the spectrum analyzer was 5 ms/division. At 1843 Hz that is about 0.1 division per cycle. That is the spacing of the "picket fence" structure. We conclude that the wave turbulence in the MHz frequency

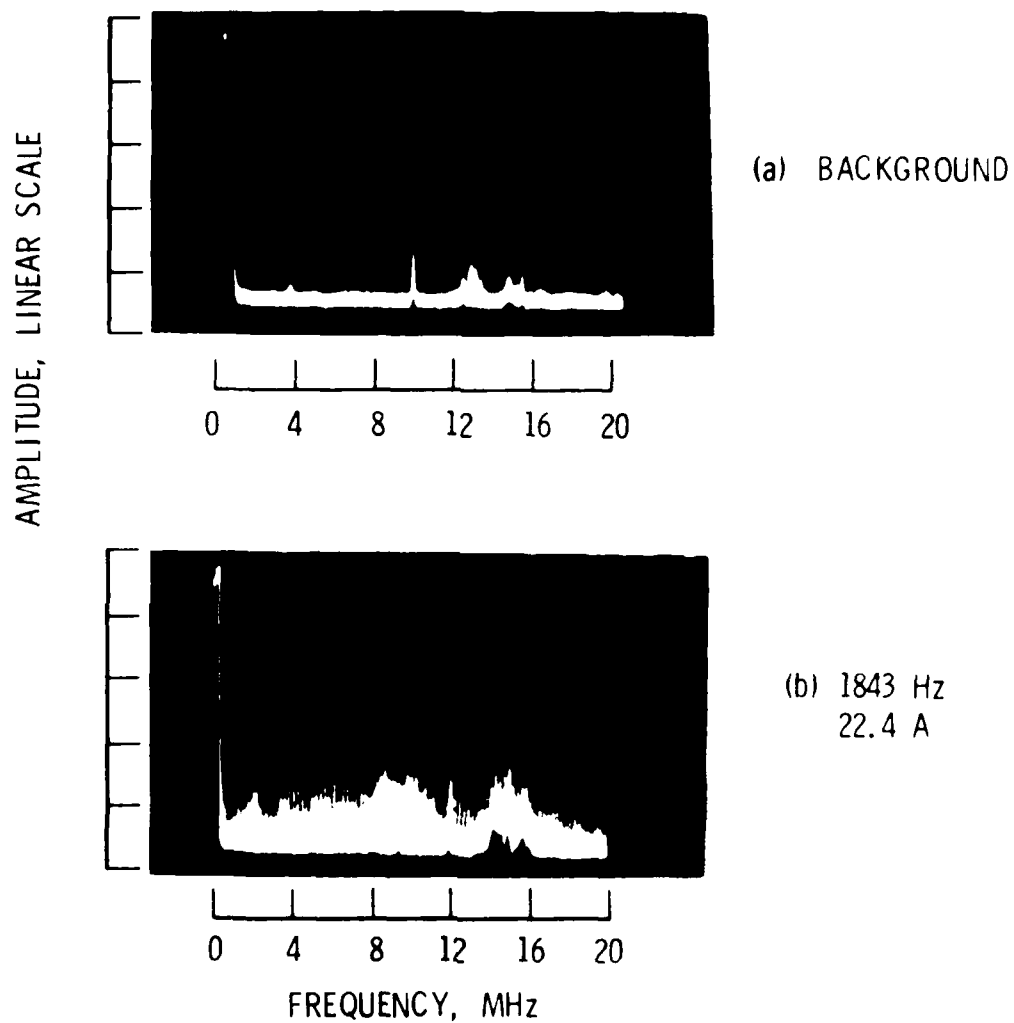


Fig. 4 Wave spectrum in plasma in the frequency range from 0 to 20 MHz. a) Background with no antenna current, b) Antenna current of 22.4 A r.m.s. at 1843 Hz.

range is being modulated almost 100% by the VLF signal on the antenna.

The increase in the circuit resistance is most likely due to power lost to plasma wave turbulence. The wave diagnostics were not designed to identify the wave modes. Scarf and Fredericks [1972] have described an energy dissipation process induced by large amplitude electric fields and by the transient production of unstable plasma distributions. These effects can not be quantitatively evaluated by theoretical analysis because the loop antenna geometry is too complex.

The a.c. magnetic field component of the near field was measured by small search coils at several locations about the antenna. The near magnetic field was directly proportional to antenna current and independent of the plasma density as expected from Ampere's law in Maxwell's equations.

Summary

A loop antenna configuration is being defined for a transmitter to radiate VLF waves within the ionosphere. A one-third scale model was tested in a space-plasma simulation chamber at NASA Lewis Research Center.

The following results were obtained:

1. The resonant frequency of the antenna circuit was insensitive to the plasma density.
2. The series resistance of the circuit increases in the plasma. This increase is small below 1 kHz and large above 3 kHz. The increased resistance is attributed to power lost to plasma turbulence.

3. The intensity of the ac magnetic-field component in the near field of the antenna in the plasma is unchanged from its value in free space.
4. The impedance of the antenna is insensitive to the rotation angle with respect to the dc magnetic field. In particular no significant impedance variations occurred at angles of 0 and 90°.

These tests confirm that a full size antenna can be tuned using fixed capacitance. The losses to be expected from plasma turbulence with the full size system cannot be readily extrapolated from the scale model tests. In particular the voltage across the terminals of the full size antenna will be significantly larger than the voltages across the terminal of the model.

References

- Baker, D. J., H. Weil and L. S. Bearce, Impedance and large signal excitation of satellite-borne antennas in the ionosphere, IEEE Trans. Antennas Propagat., AP-21(5), 672-679, 1973.
- Bell, T. F., and T. N. C. Wang, Radiation resistance of a small filamentary loop antenna in a cold multicomponent magnetoplasma, IEEE Trans. Antennas Propagat., AP-19(4), 517-522, 1971.
- Grard, R. J. L., and J. K. E. Tunaley, The impedance of the electric dipole aerial on the FR-1 satellite, Ann. Geophys., 24(1), 49-61, 1968.
- Gurnett, D. A., G. W. Pfeiffer, R. A. Anderson, S. R. Mosier and D. P. Cauffman, Initial observations of VLF electric and magnetic fields with the Injun 5 satellite, J. Geophys. Res., 74(19), 4631-4648, 1969.
- Koons, H. C., and D. A. McPherson, Measurement of the nonlinear impedance of a satellite-borne electric dipole antenna, Radio Sci. 9(5), 547-557, 1974.
- Koons, H. C., D. A. McPherson and W. B. Harbridge, Dependence of VLF electric field antenna impedance on magnetospheric plasma density, J. Geophys. Res., 75(3), 2490-2502, 1970.
- Leiphart, J. P., R. W. Zeek, L. S. Bearce and E. Toth, Penetration of the ionosphere by very-low-frequency radio signals - Interim results of the LOFTI I experiment, Proc. IRE, 50(1), 6-17, 1962.
- Scarf, F. L., and R. W. Fredricks, "Transmission losses associated with plasma perturbations," in Proceedings of the Conference on Antennas and Trans-ionospheric Propagation as related to ELF/VLF Downlink Satellite Communications, NRL Rpt. 7462, Naval Research Laboratory, Washington, D. C., p. 123-135, 1972.

- Shawhan, S. D., and D. A. Gurnett, VLF electric and magnetic fields observed with the Javelin 8.45 sounding rocket, J. Geophys. Res., 73(25), 5649-5664, 1968.
- Shkarofsky, I. P., Nonlinear sheath admittance, currents and charges associated with high peak voltage drive on a VLF/ELF dipole antenna moving in the ionosphere, Radio Sci., 7, 503-523, 1972.
- Wang, T. N. C., and T. F. Bell, On VLF radiation resistance of an electric dipole in a cold magnetoplasma, Radio Sci., 5(3), 605-610, 1970.
- Wang, T. N. C., and T. F. Bell, VLF/ELF input impedance of an arbitrarily oriented loop antenna in a cold collisionless multicomponent magnetoplasma, IEEE Trans. Antennas Propagat. (Commun.), AP-20, 394-398, 1972.

LABORATORY OPERATIONS

The Laboratory Operations of The Aerospace Corporation is conducting experimental and theoretical investigations necessary for the evaluation and application of scientific advances to new military space systems. Versatility and flexibility have been developed to a high degree by the laboratory personnel in dealing with the many problems encountered in the nation's rapidly developing space systems. Expertise in the latest scientific developments is vital to the accomplishment of tasks related to these problems. The laboratories that contribute to this research are:

Aerophysics Laboratory: Launch vehicle and reentry aerodynamics and heat transfer, propulsion chemistry and fluid mechanics, structural mechanics, flight dynamics; high-temperature thermomechanics, gas kinetics and radiation; research in environmental chemistry and contamination; cw and pulsed chemical laser development including chemical kinetics, spectroscopy, optical resonators and beam pointing, atmospheric propagation, laser effects and countermeasures.

Chemistry and Physics Laboratory: Atmospheric chemical reactions, atmospheric optics, light scattering, state-specific chemical reactions and radiation transport in rocket plumes, applied laser spectroscopy, laser chemistry, battery electrochemistry, space vacuum and radiation effects on materials, lubrication and surface phenomena, thermionic emission, photosensitive materials and detectors, atomic frequency standards, and bioenvironmental research and monitoring.

Electronics Research Laboratory: Microelectronics, GaAs low-noise and power devices, semiconductor lasers, electromagnetic and optical propagation phenomena, quantum electronics, laser communications, lidar, and electro-optics; communication sciences, applied electronics, semiconductor crystal and device physics, radiometric imaging; millimeter-wave and microwave technology.

Information Sciences Research Office: Program verification, program translation, performance-sensitive system design, distributed architectures for spaceborne computers, fault-tolerant computer systems, artificial intelligence, and microelectronics applications.

Materials Sciences Laboratory: Development of new materials: metal matrix composites, polymers, and new forms of carbon; component failure analysis and reliability; fracture mechanics and stress corrosion; evaluation of materials in space environment; materials performance in space transportation systems; analysis of systems vulnerability and survivability in enemy-induced environments.

Space Sciences Laboratory: Atmospheric and ionospheric physics, radiation from the atmosphere, density and composition of the upper atmosphere, aurorae and airglow; magnetospheric physics, cosmic rays, generation and propagation of plasma waves in the magnetosphere; solar physics, infrared astronomy; the effects of nuclear explosions, magnetic storms, and solar activity on the earth's atmosphere, ionosphere, and magnetosphere; the effects of optical, electromagnetic, and particulate radiations in space on space systems.

. . .

DATE
ILME